Automatica 47 (2011) 2534–2542

Contents lists available at SciVerse ScienceDirect

Automatica

journal homepage: www.elsevier.com/locate/automatica

Brief paper

Finite-time multi-agent deployment: A nonlinear PDE motion planning approach☆

Thomas Meurer [a,1], Miroslav Krstic [b]

[a] Automation and Control Institute, Vienna University of Technology, Gusshausstrasse 27–29, 1040 Vienna, Austria

[b] Department of Mechanical and Aerospace Engineering, University of California at San Diego, La Jolla, CA 92093-0411, USA

ARTICLE INFO

Article history:
Received 5 March 2010
Received in revised form
7 February 2011
Accepted 11 May 2011
Available online 25 September 2011

Keywords:
Motion planning
Multi-agent deployment
Flatness
Distributed-parameter systems
Formation control

ABSTRACT

The systematic flatness-based motion planning using formal power series and suitable summability methods is considered for the finite-time deployment of multi-agent systems into planar formation profiles along predefined spatial–temporal paths. Thereby, a distributed-parameter setting is proposed, where the collective leader–follower agent dynamics is modeled by two boundary controlled nonlinear time-varying PDEs governing the motion of an agent continuum in the plane. The discretization of the PDE model directly induces a decentralized communication and interconnection structure for the multi-agent system, which is required to achieve the desired spatial–temporal paths and deployment formations.

1. Introduction

In the past decades, extensive research has been conducted on the cooperative formation control of multi-agent systems with possible applications ranging from UAVs over transportation systems to micro-satellite clusters (see, e.g., Bullo, Cortés, and Martínez (2009), Murray (2007), Ren and Beard (2008) for rather recent and comprehensive overviews). Thereby, different analysis and design approaches have emerged depending on the available communication topology and the considered formation control task. In the behavior-based approach a desired set of behaviors is assigned to the individual agents and the overall behavior of the system is achieved by defining the relative importance between the individual behaviors (Balch & Arkin, 1998). The virtual structure approach relies on the consideration of the entire formation as a single (rigid) entity and the desired motion is assigned to the rigid structure (Ren & Beard, 2004). Alternatively, constraint functions relating the positions and orientations of the individual agents can be defined (Zhang & Hu, 2008). The potential field approach is based on the introduction of structural interaction forces between neighboring agents in order to stabilize the system to the equilibrium manifold (Olfati-Saber, 2006). Moreover, optimization-based approaches are analyzed to minimize the individual and cumulative formation error (Dunbar & Murray, 2006; Murray, 2007). In general, an additional distinction arises between leaderless and leader–follower systems. In the latter either a real or a virtual agent is chosen as the leader, whose motion follows a desired trajectory. The follower agents track the movement of the leader while maintaining their overall formation. Thereby in general feedback interconnection strategies are analyzed, which either rely on global or local information corresponding to a centralized or decentralized control scheme to achieve the agent deployment into prescribed formations.

Besides the discrete analysis of the interconnected individual agents, continuous models based on partial differential equations (PDEs) have been used to represent and control traffic flow (Alvarez, Horowitz, & Li, 1999) or large vehicular platoons (Barooah, Mehta, & Hespanha, 2009). In view of the analysis of multi-agent systems, Ferrari-Trecate, Buffa, and Gati (2006) introduce a semi-discrete continuous-time partial difference equation framework over graphs, where the spatial discretization corresponds to the individual agent. It is thereby shown that the graph Laplacian control proposed in Olfati-Saber and Murray (2004) coincides with the linear heat equation. To incorporate certain parameter uncertainties for multi-agent systems modeled by partial difference equations adaptive control is considered, e.g., in Kim, Kim, Natarajan, Kelly, and Bentsman (2008). A wave-like

☆ The material in this paper was partially presented at the 8th IFAC Symposium on Nonlinear Control Systems (NOLCOS 2010), September 1–3, 2010, Bologna, Italy. This paper was recommended for publication in revised form by Associate Editor Zhihua Qu under the direction of Editor Andrew R. Teel.

E-mail addresses: meurer@acin.tuwien.ac.at (T. Meurer), krstic@ucsd.edu (M. Krstic).

[1] Tel.: +43 1 58801 37627; fax: +43 1 58801 37699.

0005-1098/$ – see front matter © 2011 Elsevier Ltd. All rights reserved.
doi:10.1016/j.automatica.2011.08.045

PDE model in the limit as the number of vehicles in a platoon moving in a straight line tends to infinity in proposed in Barooah et al. (2009). With this, the stability margin of large vehicular platoons under bidirectional decentralized control was analyzed and improved by introducing a forward–backward asymmetry in the control gains. Results on connecting PDEs and distributed systems towards the evaluation of system theoretic properties are provided in Sarlette and Sepulchre (2009). In terms of formation control, linear diffusion–advection–reaction equations with dynamic boundary conditions were studied in Frihauf and Krstic (2009) to achieve the deployment into equilibrium profiles. For this, PDE backstepping (Krstic & Smyshlyaev, 2008) was applied in order to exponentially stabilize the equilibrium profiles.

In this paper, a systematic nonlinear PDE-based motion planning framework is proposed for the realization of finite-time transitions between desired deployment formations along predefined spatial–temporal paths. For this, nonlinear time-varying Burgers-like PDEs are used to represent the location of a continuum of mobile agents in the plane. The desired deployment formations correspond to the equilibrium profiles of the governing PDEs, which include shock-like effects as are well known for Burgers equation (see, e.g., also Krstic, Magnis, and Vazquez (2008, 2009) for results on their stabilization). Moreover, a leader–follower configuration is considered, where the positions or velocities, respectively, of the leader agent and another agent, subsequently referred to as the anchor agent, serve as boundary inputs. For their design, a flatness-based approach (see, e.g., Fliess, Lévine, Martin, and Rouchon (1995) for the general theory for finite-dimensional systems and, e.g., Lynch and Rudolph (2002), Petit and Rouchon (2002), Meurer and Zeitz (2005, 2008), Meurer and Kugi (2009) for extensions to PDEs) is considered, which is based on the differential parametrization of the system states and the boundary inputs in terms of a flat or so-called basic output by making use of formal power series and suitable summability methods.

The paper is organized as follows: Section 2 introduces the considered PDE-based leader-enabled deployment problem which is solved in Section 3 following a flatness-based approach. For the determination of the feedforward formation control the assignment of suitable desired trajectories is analyzed in Section 4 in view of the realization of the leader-enabled deployment into planar curves. Simulation results are presented in Section 5 and some final remarks conclude the paper.

2. PDE-based leader-enabled deployment

The leader-enabled deployment of mobile agents is considered under the assumptions that the agents are fully actuated and operate in a common reference frame. Motivated by the correspondence of graph Laplacian control and the linear heat equation in the limit as the number of interconnected agents approaches infinity (Ferrari-Trecate et al., 2006), subsequently, the planar motion of the agents in the (x^1, x^2)-domain is introduced in terms of two decoupled nonlinear heat equations in the form of modified viscous Burgers equations with time-varying parameters.

2.1. Burgers equations and continuous agent topology

The motivation to use Burgers-type equations in the deployment of a continuum of interconnected agents is twofold. To generate complex profiles involving corners (Fig. 1, left) and "switchback" shapes (Fig. 1, right), one option is to use a linear PDE model that is of high order in the spatial variable α, where α denotes the continuous index of the agents. This option creates both considerable challenges for stabilization and for actuation.

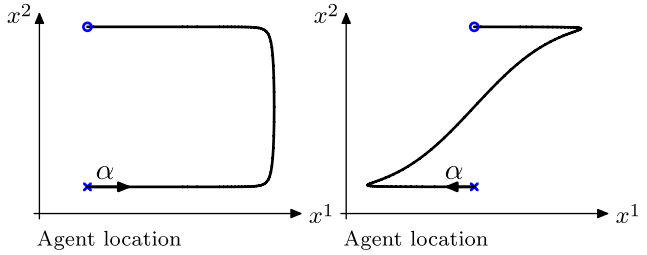

Fig. 1. Examples of deployment profiles for multi-agent continuum in the (x^1, x^2)-plane with the α-coordinate representing the continuous communication path. Anchor and leader agents are marked by $\times$ and $\circ$.

With regards to stabilization, linear Korteweg–de Vries (third order), Kuramoto–Sivashinsky (fourth order), and higher-order PDEs are much harder to stabilize than parabolic PDEs. With regards to actuation, higher numbers of derivatives in α in the PDE require to employ a higher number of boundary conditions, meaning, a higher number of leaders and anchors.

The second option is to stick with PDEs that are second-order in α, namely, parabolic, but allow nonlinearities, such as in the Burgers equation. The quadratic nonlinearity in the Burgers equation, which generates shock-like equilibrium profiles, allows for corner-like shapes in deployment profiles. At the same time, the motion planning and stabilization problems for Burgers equation are tractable, with a number of boundary conditions/inputs that is no higher than for linear parabolic PDEs.

Thus, the Burgers equation is a natural choice for considerably expanding the catalog of achievable deployment profiles, without dramatically expanding the complexity of the problem of deploying the agents to the desired profile.

We consider an agent continuum in the (x^1, x^2)-plane (cf. Fig. 1) with the communication path represented by the continuous independent coordinate $\alpha \in [0, 1]$ referring to the agent index in the continuum. The locations of the anchor and leader agents at $\alpha = 0\,(\times)$ and $\alpha = 1\,(\circ)$ serve as inputs, whose temporal paths are determined by flatness-based motion planning and feedforward control. Each $x^j = x^j(\alpha, t)$, $j = 1, 2$, is thereby governed by a boundary controlled PDE, which determines the individual motion of the agent continuum in the x^j-direction. By superimposing the respective x^1- and x^2-contributions, the desired planar deployment is achieved along prescribed spatial–temporal motion paths. The PDE formulation thereby in particular enables a design, which is independent of the actual communication topology. The latter is induced by means of a finite difference discretization scheme to transfer the results from an agent continuum to a discrete set of agents, where any follower agent processes only local information.

2.2. Distributed-parameter agent dynamics

As pointed out above, in the following a modified viscous Burgers equation is considered to model the motion of the mobile agent continuum with respect to the $x^j(\alpha, t)$-coordinate, $j \in \{1, 2\}$, i.e.

$$\partial_t x^j(\alpha, t) = a^j \partial_\alpha^2 x^j(\alpha, t) - b^j x^j(\alpha, t) \partial_\alpha x^j(\alpha, t) + c^j(t) x^j(\alpha, t), \quad \alpha \in (0, 1), t \in \mathbb{R}_{t_0} \tag{1a}$$

with $a^j, b^j > 0$, the time-varying parameter $c^j(t) \in \mathbb{R}$, and $\mathbb{R}_{t_0} = \{t \in \mathbb{R} \mid t > t_0\}$. The independent coordinate α corresponds to an agent index in a large group (continuum) of agents. The positions of the anchor agent ($\alpha = 0$) and the leader agent ($\alpha = 1$) are governed by the inhomogeneous Dirichlet boundary conditions

$$x^j(0, t) = u_a^j(t), \qquad x^j(1, t) = u_l^j(t), \quad t > t_0. \tag{1b}$$

Note that velocity inputs can be equivalently included in the analysis. The initial condition follows as

$$x^j(\alpha, t_0) = x_0^j(\alpha), \quad \alpha \in [0, 1] \tag{1c}$$

with $x_0^j(\alpha)$ an initial steady state formation profile. In the following, the motion planning problem is considered based on (1) to realize the finite-time deployment of the agents into desired formations governed by the steady state solutions of the modified Burgers equation along suitable predefined spatial–temporal transition paths.

2.3. Desired deployment profiles

Besides the semilinearity of the PDE (1a) the steady state analysis becomes more involved due to the time-variance induced by the parameter $c^j(t)$. In particular, stationarity at $t = \bar{t} \geq t_0$ requires that the following boundary-value problem is satisfied, i.e.

$$a^j \partial_\alpha^2 \bar{x}^j(\alpha) - b^j \bar{x}^j(\alpha) \partial_\alpha \bar{x}^j(\alpha) + c^j(t) \bar{x}^j(\alpha) = 0 \tag{2a}$$

$$\bar{x}^j(0) = \bar{u}_a^j, \qquad \bar{x}^j(1) = \bar{u}_l^j. \tag{2b}$$

Here, $\bar{u}_a^j$ and $\bar{u}_l^j$ denote constant input values and for $\bar{x}^j(\alpha) \neq 0$ the parameter $c^j(t)$ has to fulfill $c^j(t) = \bar{c}^j$ while $\partial_t^n c^j(t) = 0$, $n \geq 1$, for $t \geq \bar{t}$. The latter conditions imply that $c^j(t)$ is non-analytic at $t = t_0$. If Eqs. (2) are satisfied $\bar{x}^j(\alpha; \bar{c}^j, \bar{u}_a^j, \bar{u}_l^j) = \bar{x}^j(\alpha)$ is called a stationary or steady state profile. Subsequently, desired formation profiles for the agent continuum are determined by the superposition of steady states $(\bar{x}^1(\alpha), \bar{x}^2(\alpha))$ in the x^1- and x^2-direction. Thereby, depending on the system parameters and the stationary anchor and leader positions, a broad variety of solutions to (2) can be obtained in view of the solution of the deployment problem.

For general parameter sets $(a^j, b^j, \bar{c}^j)$, the solution to (2) has to be computed numerically by prescribing both $\bar{u}_a^j$ and $\bar{u}_l^j$. However, an analytical analysis is possible for special cases. For the linear set-up with $b^j = 0$, subsequently, two distinct families of steady state solutions are considered, i.e.

$$\bar{x}^j(\alpha; \bar{c}^j, \bar{u}_a^j, \bar{u}_l^j) = \bar{u}_a^j + \alpha \left(\bar{u}_l^j - \bar{u}_a^j \right) \tag{3a}$$

for $\bar{c}^j = 0$ and

$$\bar{x}^j(\alpha; \bar{c}^j, \bar{u}_a^j, \bar{u}_l^j) = A \sin(k\pi\alpha), \quad \forall A \in \mathbb{R} \tag{3b}$$

given $\bar{c}^j = (k\pi)^2$, $k \in \mathbb{N}$, and $\bar{u}_a^j = \bar{u}_l^j = 0$. Further solutions to (2) for $b^j = 0$ are, e.g., summarized in Frihauf and Krstic (2009). If $b^j \neq 0$, solutions to (2) are determined, e.g., in Krstic et al. (2009) and illustrate the well-known appearance of shock-like profiles for viscous Burgers equation. In combination with numerical routines for the solution of boundary-value problems a computational framework can be hence introduced to characterize desired formation profiles depending on the system parameters $(a^j, b^j, \bar{c}^j)$ and the stationary anchor and leader positions.

Obviously, if $c^j(t)$ involves points of non-analyticity at $t \in \{t_1, t_2, \ldots, t_l\}$, the set of achievable deployment profiles is significantly enlarged, which can be exploited for motion planning to enable the finite time transitions between different families of steady states.

3. Flatness-based motion planning

For the solution of the finite time deployment problem into desired formation profiles, subsequently flatness-based methods are applied for the determination of suitable spatial–temporal transition paths and the corresponding input trajectories for the anchor and leader.

3.1. Formal power series solution

By assuming that $x^j(\alpha, t)$ can be represented in terms of a formal power series, i.e. $x^j(\alpha, t) \to \hat{x}^j(\alpha, t)$, where

$$\hat{x}^j(\alpha, t) = \sum_{n=0}^{\infty} \hat{x}_n^j(t) \frac{(\alpha - \hat{\alpha})^n}{n!} \tag{4}$$

with $\hat{\alpha} \in (0, 1)$ fixed but arbitrary and the consideration of the Cauchy product formula for the evaluation of the nonlinear term $x^j(\alpha, t)\partial_\alpha x^j(\alpha, t)$, the substitution of $\hat{x}^j(\alpha, t)$ into the PDE (1a) yields the following second order differential recursion for the series coefficients

$$\hat{x}_n^j(t) = \frac{1}{a^j} \left(b^j \sum_{i=0}^{n-2} \binom{n-2}{i} \hat{x}_{n-2-i}^j(t) \hat{x}_{i+1}^j(t) - c^j(t) \hat{x}_{n-2}^j(t) + \partial_t \hat{x}_{n-2}^j(t) \right), \quad n \geq 2 \tag{5a}$$

$$\hat{x}_0^j(t) = \hat{x}^j(\hat{\alpha}, t) = y_1^j(t) \tag{5b}$$

$$\hat{x}_1^j(t) = \partial_\alpha \hat{x}^j(\hat{\alpha}, t) = y_2^j(t). \tag{5c}$$

For the evaluation of the two starting conditions (5b) and (5c) the functions $y_1^j(t)$ and $y_2^j(t)$ are introduced, which serve as degrees of freedom to solve the motion planning task. Obviously, the nonlinearity prevents a closed-form solution of the differential recursion. However, it can be easily shown that any series coefficient can be formally represented as

$$\hat{x}_n^j(t) = \psi_n \left(\boldsymbol{y}_{1,\bar{n}(n)}^j(t), \boldsymbol{y}_{2,\bar{n}(n)}^j(t) \right)$$

with $\bar{n}(n) = (n - n \bmod 2)/2 \in \mathbb{N}_0$. Here, the formal dependencies are summarized as

$$\boldsymbol{y}_{i,\bar{n}(n)}^j(t) = [y_i^j(t), \partial_t y_i^j(t), \ldots, \partial_t^{\bar{n}(n)} y_i^j(t)]^T, \quad i = 1, 2.$$

With this, both the state and inputs can be schematically parametrized as

$$x^j(\alpha, t) = \sum_{n=0}^{\infty} \psi_n \left(\boldsymbol{y}_{1,\bar{n}(n)}^j(t), \boldsymbol{y}_{2,\bar{n}(n)}^j(t) \right) \frac{(\alpha - \hat{\alpha})^n}{(n)!} \tag{6a}$$

$$u_a^j(t) = \sum_{n=0}^{\infty} \psi_n \left(\boldsymbol{y}_{1,\bar{n}(n)}^j(t), \boldsymbol{y}_{2,\bar{n}(n)}^j(t) \right) \frac{(-\hat{\alpha})^n}{(n)!} \tag{6b}$$

$$u_l^j(t) = \sum_{n=0}^{\infty} \psi_n \left(\boldsymbol{y}_{1,\bar{n}(n)}^j(t), \boldsymbol{y}_{2,\bar{n}(n)}^j(t) \right) \frac{(1 - \hat{\alpha})^n}{(n)!} \tag{6c}$$

in terms of $y_1^j(t)$, $y_2^j(t)$, and their time-derivatives. In accordance with the common notation for finite-dimensional nonlinear systems, the tuple $(y_1^j(t), y_2^j(t))$ is denoted a flat or basic output for (1). The determined expressions are so far only formal. Hence, to deduce meaningful expressions from (6) the uniform convergence of the parametrized formal power series has to be analyzed, which, as is shown below, results in a problem of trajectory planning for the basic output.

3.2. Uniform convergence in Gevrey classes

For convergence analysis, the notion of a Gevrey class is required (Rodino, 1993).

Definition 1 (*Gevrey class*)**.** The function $f(t)$ is in $G_{M,\varsigma}(\Omega)$, the Gevrey class of order ς in Ω, if $f(t) \in \mathcal{C}^\infty(\Omega)$ and there exist a positive constant M such that

$$\sup_{t \in \Omega} |\partial_t^n f(t)| \leq M^{n+1} (n!)^\varsigma \quad \forall n \in \mathbb{N}_0. \tag{7}$$

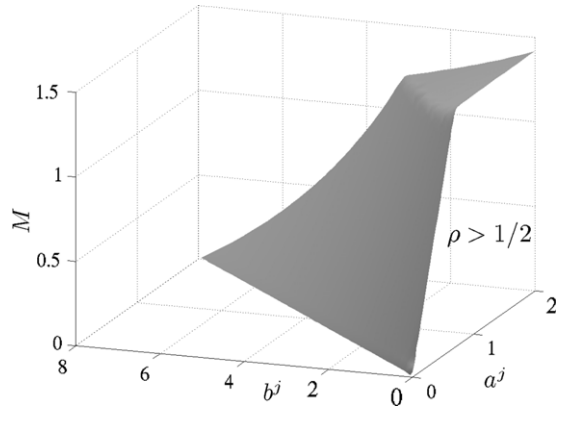

Fig. 2. Domain of convergence governed by $\rho = 1/(MA_j(M)) > 1/2$ in the (a^j, b^j, M)-domain.

If $\varsigma < 1$, the function is entire while it is analytic for $\varsigma = 1$ and non-analytic if $\varsigma > 1$. With this, the following assumption is imposed on the parameter $c^j(t)$, which implies that $c^j(t)$ is smooth but locally non-analytic as suggested in Section 2.3.

Assumption 2. The function $c^j(t) \in G_{M_c,\varsigma}(\overline{\mathbb{R}_{t_0}})$ with $\varsigma \in (1, 2]$.

The proof of uniform series convergence essentially relies on the determination of a suitable bound on the parametrized series coefficients (5) (see, e.g., Lynch and Rudolph (2002), Meurer and Zeitz (2005), Meurer and Zeitz (2008) for related results). However, certain modifications are required due to the considered configuration involving multiple input functions. By restricting both the tuple $(y_1^j(t), y_2^j(t))$ and $c^j(t)$ to certain Gevrey classes the main result can be formulated as follows.

Theorem 3. *Let $y_1^j(t), y_2^j(t) \in G_{M_y,\varsigma}(\overline{\mathbb{R}_{t_0}})$ with $\varsigma \in [1, 2]$ and let $c^j(t) \in G_{M_c,\varsigma}(\overline{\mathbb{R}_{t_0}})$ be as in Assumption 2. Then the series (6a) has a radius of convergence $\rho = 1/(MA_j(M))$ in $|\alpha - \hat{\alpha}|$, where $M = \max\{M_y, M_c\}$ with Gevrey constants $M_y, M_c > 0$ and*

$$A_j(M) = \max\left\{1, \sqrt{\frac{2+b^j}{2a^j}}, \frac{b^j}{6a^j}\left(1+\frac{3}{2M}\right) + \sqrt{\left(\frac{b^j}{6a^j}\left(1+\frac{3}{2M}\right)\right)^2 + \frac{2}{Ma^j}}\right\}. \tag{8}$$

For a proof, consult Appendix A. It is obvious from (8) that the domain of convergence decreases for decreasing a^j and approaches zero for $a^j \to 0$. This is exemplarily illustrated in Fig. 2. Here, the domain of convergence fulfilling the condition $\rho > 1/2$ given $\hat{\alpha} = 1/2$ is depicted in the (a^j, b^j, M)-domain. Note that the figure continues to a semi-bounded domain along the direction of the a^j-axis. Obviously for decreasing a^j, the domain of convergence decreases and approaches zero for $a^j \to 0$. This implies that the shock-like effects, which appear for $a^j \ll 1$ can be only represented by the determined power series in a small subregion of the α-axis. Hence, in order to capture and realize shock-like profiles for all $\alpha \in [0, 1]$ suitable summability methods have to be integrated for the evaluation of the parametrization.

Remark 4 (*Uniform Convergence for $b^j = 0$*)**.** For the linear case with $b^j = 0$ it can be shown by induction that the parametrized series coefficients satisfy $|\partial_t^l \hat{x}_n^j(t)| \le M^{l+1}F^n((l+n)!)^\varsigma/(n!)^{\varsigma/2}$ for some $F > 0$ given $y_1^j(t), y_2^j(t) \in G_{M,\varsigma}(\overline{\mathbb{R}_{t_0}})$ with $\varsigma \in [1, 2]$. By making use of the Cauchy–Hadamard theorem an infinite radius of convergence is thus obtained for $\varsigma < 2$.

3.3. Summability methods

The previous results directly illustrate that the convergence of the power series (6a) determining the state and input parametrization for the modified Burgers equation (1) in terms of the basic output greatly depends on the appropriate trajectory assignment for the basic output and the system parameters. In order to overcome these convergence limitations so-called summability methods provide a powerful tool to prolong the space of uniformly convergent power series in order to deal with certain divergent series. For a comprehensive discussion the reader is referred, e.g., to Hardy (1964) and Balser (2000) and the references therein. Thereby, rather general results are mainly available for formal solutions to ordinary differential equations (ODEs) (Balser, 2000) with certain extensions to PDEs (Balser, 2001; Balser & Miyake, 1999). One promising technique, which is applicable to both ODEs and PDEs is provided by the so-called k-summation. Given the formal power series (4) k-summation can be introduced as

$$x^j(\alpha, t) \cong \hat{x}^j(\alpha, t) = (\mathcal{S}_B^k \hat{x}^j)(\alpha, t) \tag{9}$$

with

$$\left(\mathcal{S}_B^k \hat{x}^j\right)(\alpha, t) = \lim_{\xi \to \infty} \sum_{n=0}^{\infty} s_n(\alpha, t) \frac{\xi^n}{\Gamma\left(1+\frac{n}{k}\right)} / E_\infty^k(\xi)$$

and the partial sum $s_n(\alpha, t) = \sum_{l=0}^n \hat{x}_l^j(t)(\alpha - \hat{\alpha})^l/l!$ as well as $E_n^k(\xi) = \sum_{l=0}^n \xi^l/\Gamma(1 + l/k)$ (Balser & Braun, 2000). In view of the application of k-summation to formal power series solutions arising from PDE control problems, it has to be noted that many problems typically allow only the determination of a finite number of series coefficients, which hence requires an appropriate modification of the previously introduced concept. This leads to an interpretation in terms of so-called generalized sequence transformations (Weniger, 1989), which play an important role in quantum physics and quantum chemistry and allow us to accelerate convergence and approximate the sum of certain divergent series using only partial information. Within this framework, a modification of the previously discussed k-summation in the form (9), namely the so-called (N, ξ)-approximate k-summation, is proposed (Meurer, 2005), i.e.

$$\left(\mathcal{S}_k^{N,\xi} \hat{x}\right)(\alpha, t) = \sum_{n=0}^{N} s_n(\alpha, t) \frac{\xi}{\Gamma\left(1+\frac{n}{k}\right)} / E_N^k(\xi). \tag{10}$$

This method can be applied to extract the limit (in the sense of the summability method) of the slowly converging or possibly diverging series (4) from a finite number of series coefficients depending on the appropriate choice of the summation parameters ξ and k. The interested reader is referred to Meurer (2005), Meurer and Zeitz (2005, 2008) for a detailed study of summation techniques in view of tracking control design for nonlinear parabolic PDEs and the appropriate choice of the summation parameters.

4. Trajectory assignment and feedforward formation control

The flatness-based state and input parametrizations provide a systematic approach for the solution of the motion planning problem to realize the finite-time deployment of a continuum of agents into the desired formation profiles summarized in Section 2.3. This requires us to determine appropriate trajectories for the basic output $(y_1^j(t), y_2^j(t))$ in view of the convergence results and the summability properties. Thereby, the time-varying parameter $c^j(t)$ plays a crucial role and serves as a degree of freedom, whose careful selection allows the transition between different families of formation profiles.

4.1. Connecting families of steady state formations

As pointed out in Section 2.3, the existence of steady state solutions to the modified time-varying Burgers equation relies on the non-analyticity of the time-varying parameter $c^j(t)$, i.e. $\exists\, \bar{t} \geq t_0 : c^j(\bar{t}) = \overline{c}^j$ and $\partial_t^n c^j(t)|_{t=\bar{t}} = 0, \forall n \geq 1$. To address this, subsequently the function

$$c^j(t) = \overline{c}^{j,0} + \left(\overline{c}^{j,1} - \overline{c}^{j,0}\right) \Phi_{\gamma_c^j, T_c^j}(t - t_0) \tag{11}$$

is considered, where

$$\Phi_{\gamma,T}(t) = \begin{cases} 0, & t \leq 0 \\ 1, & t \geq T \\ \dfrac{\int_0^t \Lambda_{\gamma,T}(\tau)\mathrm{d}\tau}{\int_0^T \Lambda_{\gamma,T}(\tau)\mathrm{d}\tau}, & t \in (0,T) \end{cases} \tag{12}$$

and $\Lambda_{\gamma,T}(t) = 0$ if $t \notin (0,T)$ and $\Lambda_{\gamma,T}(t) = \exp(-[(1 - t/T)t/T]^{-\gamma})$ for $t \in (0,T)$. The smooth compact support function $\Phi_{\gamma,T}(t)$, $\gamma > 0$ is non-analytic at $t \in \{0,T\}$ with $\partial_t^k \Phi_{\gamma,T}(t) = 0$ for all $t \leq 0$ and $t \geq T$ with $k \in \mathbb{N}$. Furthermore, $\Phi_{\gamma,T}(t)$ is of Gevrey order $\varsigma = 1 + 1/\gamma$ (Rodino, 1993). Hence, by adjusting the constants $\overline{c}^{j,0}$ and $\overline{c}^{j,T}$ it follows immediately that (1) exhibits two families of steady states satisfying (2) with $c^j(t) = \overline{c}^{j,0}$ for $t \leq t_0$ and with $c^j(t) = \overline{c}^{j,1}$ for $t \geq t_0 + T_c^j$, respectively, which are connected by the path $c^j(t)$.

4.2. Trajectory assignment for the basic output

For the assignment of a tuple of desired trajectories $t \mapsto (y_1^{*,j}(t), y_2^{*,j}(t))$ to realize transitions between desired formation profiles within a prescribed time-interval $t \in [t_0, t_0 + T^j]$, $0 < T_c^j \leq T^j$, it is required to take into account that both $y_1^{*,j}(t)$ and $y_2^{*,j}(t)$ have to be locally non-analytic at $t = t_0$ and $t = t_0 + T^j$ to ensure the compatibility with the stationarity conditions. In view of Definition 1 this implies that necessarily $y_i^{*,j}(t) \in G_{M,\varsigma}(\overline{\mathbb{R}_{t_0}})$, $i = 1, 2$, with $\varsigma \in (1, 2]$. Therefore, consider

$$y_1^{*,j}(t) = A_1^{j,0} + (A_1^{j,1} - A_1^{j,0}) \Phi_{\gamma_1^j, T^j}(t - t_0) \tag{13a}$$

$$y_2^{*,j}(t) = A_2^{j,0} + (A_2^{j,1} - A_2^{j,0}) \Phi_{\gamma_2^j, T^j}(t - t_0) \tag{13b}$$

with $\Phi_{\gamma,T}(\cdot)$ as introduced in (12). The constants $A_i^{j,0}$ and $A_i^{j,1}$, $i = 1, 2$, can be determined depending on the desired initial and final formation profile corresponding to the steady states governed by (2). For this, let $\overline{x}^j(\hat{\alpha}; \overline{c}^{j,0}, \overline{u}_a^{j,0}, \overline{u}_l^{j,0})$ and $\overline{x}^j(\hat{\alpha}; \overline{c}^{j,1}, \overline{u}_a^{j,1}, \overline{u}_l^{j,1})$ denote a desired initial and final steady state for $t \leq t_0$ and $t \geq t_0 + T^j$, respectively, which in general belong to different families of steady states. In view of the starting conditions (5b) and (5c) this implies that

$$\begin{aligned} A_1^{j,0} &= y_1^{*,j}(t_0) = \overline{x}^j(\hat{\alpha}; \overline{c}^{j,0}, \overline{u}_a^{j,0}, \overline{u}_l^{j,0}), \\ A_2^{j,0} &= y_2^{*,j}(t_0) = \partial_\alpha \overline{x}^j(\hat{\alpha}; \overline{c}^{j,0}, \overline{u}_a^{j,0}, \overline{u}_l^{j,0}) \\ A_1^{j,1} &= y_1^{*,j}(t_0 + T^j) = \overline{x}^j(\hat{\alpha}; \overline{c}^{j,1}, \overline{u}_a^{j,1}, \overline{u}_l^{j,1}), \\ A_2^{j,1} &= y_2^{*,j}(t_0 + T^j) = \partial_\alpha \overline{x}^j(\hat{\alpha}; \overline{c}^{j,1}, \overline{u}_a^{j,1}, \overline{u}_l^{j,1}). \end{aligned} \tag{14}$$

As a result, once the desired stationary positions of the anchor and the leader are assigned the respective desired trajectories for the basic output, which determine the spatial–temporal connection path between the initial and final formation profile according to (6), are directly obtained from (13) with (14).

Remark 5. The previous results can be further generalized by considering a sequence of $N+1$ transitions between $N+1$ desired formation profiles possibly belonging to $N+1$ different families of steady states $\overline{x}^j(\alpha; \overline{c}^{j,p}, \overline{u}_a^{j,p}, \overline{u}_l^{j,p})$, $p = 0, 1, \ldots, N$. For this, the path

$$\begin{aligned} c^j(t) = \overline{c}^{j,0} &+ \sum_{p=0}^{N-1} (\overline{c}^{j,p+1} - \overline{c}^{j,p}) \\ &\times \Phi_{\gamma_{c,p+1}^j, T_{c,2p+1}^j - T_{c,2p}^j}\left(t - t_0 - T_{c,2p}^j\right) \end{aligned}$$

together with the desired basic output trajectory

$$\begin{aligned} y_i^{*,j}(t) = A_i^{j,0} &+ \sum_{p=0}^{N-1} (A_i^{j,p+1} - A_i^{j,p}) \\ &\times \Phi_{\gamma_{p+1}^j, T_{2p+1}^j - T_{2p}^j}(t - t_0 - T_{2p}^j), \quad i = 1, 2 \end{aligned}$$

have to be assigned. Here, $0 = T_0^j = T_{c,0}^j < T_{c,1}^j \leq T_1^j < \cdots < T_{c,2N-2} \leq T_{2N-2}^j$ and the constants A_i^p follow from

$$\begin{aligned} A_1^{j,p} &= \overline{x}^j(\hat{\alpha}; \overline{c}^{j,p}, \overline{u}_a^{j,p}, \overline{u}_l^{j,p}) \\ A_2^{j,p} &= \partial_\alpha \overline{x}^j(\hat{\alpha}; \overline{c}^{j,p}, \overline{u}_a^{j,p}, \overline{u}_l^{j,p}) \end{aligned}$$

for $p = 0, 1, \ldots, N$. With this, the $0 < p$-th steady state formation profile is reached at $t_p = t_0 + T_{2p-1}$ and is held for the period $T_{2p} - T_{2p-1}$.

4.3. Feedforward formation control

As a result, the evaluation of the parametrizations (6) with $c^j(t)$ assigned in terms of (11) and $(y_1^j(t), y_2^j(t))$ replaced by $(y_1^{*,j}(t), y_2^{*,j}(t))$ yields the corresponding feedforward controls $u_a^{*,j}(t)$ and $u_l^{*,j}(t)$ for the anchor and leader, respectively, to realize the transient spatial–temporal formation $x^{*,j}(\alpha, t)$. However, in view of Theorem 3 it can be expected that the resulting series are in general divergent such that subsequently the (N, ξ)-approximate k-summation as introduced in (10) with suitable parameters N and ξ depending on the system parameters a^j, b^j, $c^j(t)$ and the properties of $(y_1^{*,j}(t), y_2^{*,j}(t))$ is considered for the evaluation of the feedforward controls (6b) and (6c), i.e.

$$u_a^{*,j}(t) = \left(\mathcal{S}_k^{N,\xi}\hat{x}\right)(0,t), \qquad u_l^{*,j}(t) = \left(\mathcal{S}_k^{N,\xi}\hat{x}\right)(1,t). \tag{15}$$

To apply the presented results for a continuum of agents governed by the nonlinear distributed-parameter system (1) to a finite-dimensional set of agents, a discretization of the PDE with respect to the α-coordinate is introduced, which directly induces a certain communication and feedback topology (see also Frihauf & Krstic, 2009).

4.4. PDE discretization, communication topology, and agent interconnection

As pointed out in Section 2.1, the continuous PDE formulation yields a motion planning framework, which is independent of the actual communication topology. By spatially discretizing the PDE, a decentralized communication structure is imposed, which is shown in Fig. 3 for the example of a three-point discretization scheme. The interconnection between the individual agents is thereby determined by the structure of the distributed-parameter systems (1) governing the collective motion of the agents in the (x^1, x^2)-plane.

Hence, let $x_i^j(t) = x^j(i\Delta\alpha, t)$ for $i = 0, 1, \ldots, m$, with $\Delta\alpha = 1/m$, where $m+1$ denotes the number of agents. With this, the

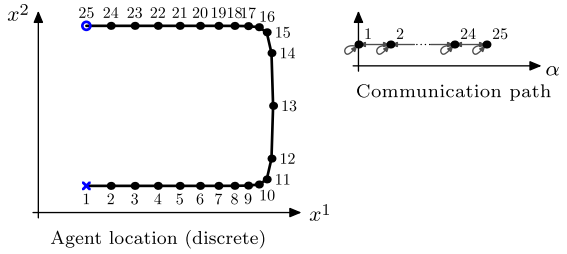

Fig. 3. Communication topology imposed by spatial discretization for the example of 25 agents in the plane. Anchor, leader, and follower agents are marked by ×, ∘, and •.

discretization of (1) using second order finite differences results in

$$\partial_t x_i^j(t) = \frac{2a^j - b^j \Delta\alpha x_i^j(t)}{2\Delta\alpha^2} x_{i+1}^j(t) + \left(c^j(t) - \frac{2a^j}{\Delta\alpha^2}\right) x_i^j(t) + \frac{2a^j + b^j \Delta\alpha x_i^j(t)}{2\Delta\alpha^2} x_{i-1}^j(t), \quad i = 1, \ldots, m-1 \tag{16}$$

with $x_0^j(t) = u_a^{*,j}(t)$ and $x_m^j(t) = u_l^{*,j}(t)$ and the respective initial conditions $x_i^j(0) = x_0^j(i\Delta\alpha)$. From (16) it follows on the one hand that the time-varying communication and interconnection (feedback) topology, which is required to realize the desired spatial–temporal deployment paths, is directly induced by the considered discretization scheme. For the present choice resulting in a finite-dimensional system of coupled nonlinear time-varying ODEs, each follower agent requires the position information of its neighboring nodes while the positions of the anchor and the leader are imposed by the feedforward controls (15). Note that the time-variance in terms of $c^j(t)$ serves as a design parameter which is a priori known and can be hence included in each agent's configuration using, e.g., (11). This, however, relies on the time-synchronous operation using a common clock with $c^j(t)$ being either directly prescribed for all t or being initiated by transmitting the trajectory parameters $\bar{c}^{j,0}$, $\bar{c}^{j,1}$, γ_c^j, and T_c^j at certain instances of time.

On the other hand, a discretization error of the order $O(\Delta\alpha^2)$ is introduced such that the application of $u_a^{*,j}(t)$ and $u_l^{*,j}(t)$ only results in the approximate realization of the desired transition path between the initial and final formation profiles. Nevertheless, the approximation error and hence the deviation between the desired position $x_i^{*,j}(t) = x^{*,j}(i\Delta\alpha, t)$ and the actual position $x_i^j(t)$, $i = 1, \ldots, m-1$ can be reduced by increasing the number of agents $m+1$. This illustrates that the proposed PDE-based approach is particularly useful for the solution of the motion planning problem for a large number of agents. Alternatively, given a fixed number of agents the discretization error can be reduced by considering a different discretization approach such as higher-order finite differences, which in contrast imposes a different communication and interconnection topology, where in general not only the information from neighboring nodes will be required for the realization.

5. Simulation results

In the following, the application of the determined feedforward formation control is considered in three different simulation scenarios for the deployment of 25 ($m = 24$) agents into planar curves with the interconnection structure according to (16), which also serves as the simulation model. For this, the PDE-based feedforward formation control laws (15) are evaluated for $\hat{\alpha} = 1/2$ using the summation parameters summarized in Table 1 for different desired formation profiles in order to realize a finite time transition from an initial formation profile at $t = t_0 = 0$ to a final formation profile at $t = T = \max\{T^1, T^2\}$. The formation profiles are governed by the boundary-value problem (2). The system parameters a^j and b^j, the parameters of the function $c^j(t)$ according to (11) with $\gamma_c^1 = \gamma_c^2 = 2$, and the respective anchor and leader positions $\bar{u}_a^j$, $\bar{u}_l^j$, $j = 1, 2$ at $t = T$ are thereby summarized in Table 1 for each scenario. The initial anchor and leader positions at $t = t_0$ are exemplarily chosen as $(\bar{u}_a^{1,0}, \bar{u}_a^{2,0}) = (-1, 0)$ and $(\bar{u}_l^{1,0}, \bar{u}_l^{2,0}) = (1, 0)$. The transition trajectories for the basic outputs are assigned according to (13) with (14) and the parameters $\gamma_i^j = \gamma = 1.2$, $i, j = 1, 2$, such that both $y_1^{*,j}(t)$ and $y_2^{*,j}(t)$ are of Gevrey order $\varsigma = 1 + 1/\gamma = 1.83$.

In the first scenario S_1, the desired formation profiles and the transition dynamics in both directions are governed by a linear diffusion–reaction equation since $b^1 = b^2 = 0$. For the considered set of parameters as well as anchor and leader positions, the initial and final profile in the x^1-direction are governed by (3a) and $\cos(2\pi\alpha)$ and in the x^2-direction similarly by (3a) but (3b) for $k = 2$, $\bar{u}_a^{2,1} = \bar{u}_l^{2,1} = 0$, respectively. The simulation results are shown in Fig. 4(a) in the (x^1, x^2)-plane with time t as a curvature parameter (top) and in the (x^1, x^2, t)-domain (bottom). These in particular illustrate the effect of the time-varying but locally non-analytic function $c^j(t)$, which allows us to obtain transition paths connecting different families of steady state profiles. For this setting the uniform convergence of the parametrized series (6) with an infinite radius of convergence is ensured by Remark 4. Hence, the application of the feedforward formation control results in the deployment of the agents starting from the straight line $x^1 \in [-1, 1]$, $x^2 = 0$ at $t = 0$ into the depicted circle at $t = 0.25$. In addition it should be pointed out that since the transition paths $x_i^{*,j}(t)$ or $x^{*,j}(i\Delta\alpha, t)$, respectively, are a priori known, their representation in the (x^1, x^2, t)-domain allows us to identify possible collisions, which can however be avoided by re-planning the desired paths $(y_1^{*,j}(t), y_2^{*,j}(t))$.

More complex deployment profiles can be realized by the combination of a linear time-varying PDE and viscous Burgers equation in the x^1- and x^2-direction, respectively. This is exemplarily shown in Fig. 4(b) and (c) for the scenarios S_2 and S_3. The distinction arises from the different parameter sets assigned for $c^1(t)$, where $\bar{c}^{1,1} = \pi^2$ in S_2 while $\bar{c}^{1,1} = 4\pi^2$ in S_3. As already pointed out above the local non-analyticity of $c^1(t)$ enables us to realize finite time transitions between different families of steady state formation profiles. Similar to the linear scenario S_1, the uniform convergence of the parametrized series for the linear x^1-PDE is guaranteed by Remark 4. However, a divergent behavior of the parametrizations for the Burgers equation can be observed such that the determination of the feedforward formation control $(u_a^{*,2}(t), u_l^{*,2}(t))$ essentially relies on the incorporation of the (N, ξ)-approximate k-summation (10) with summation parameters ξ^2 and k^2. For their determination it is herein sufficient to analyze the steady state accuracy of the feedforward controls (15). Their evaluation for different ξ^2 and k^2 at $t = T^2$, where by definition $\partial_t^n y_1^2(T^2) = \partial_t^n y_2^2(T^2) = 0$ for $n \geq 1$, and the comparison with the desired anchor and leader locations $\bar{u}_a^{2,1}$ and $\bar{u}_l^{2,1}$ directly yields a simple graphical procedure for the determination of the summation parameters. Alternative selection criteria are, e.g., formulated in Meurer (2005) by making use of graphical analysis or optimization techniques. By combining the resulting individual anchor and leader trajectories $(u_a^{*,1}(t), u_l^{*,1}(t))$ and $(u_a^{*,2}(t), u_l^{*,2}(t))$ the horseshoe-like final formation shown in Fig. 4(b) is achieved at $t = T$. By altering the reaction parameter from $\bar{c}^{1,1} = \pi^2$ to $\bar{c}^{1,1} = 4\pi^2$ such that the final steady state formation profile in the x^1-direction reads as $\bar{x}^{1,T}(\hat{\alpha}) = \sin(2\pi\alpha)$ the transition into the "switchback"-shaped final formation profile shown in Fig. 4(c) is

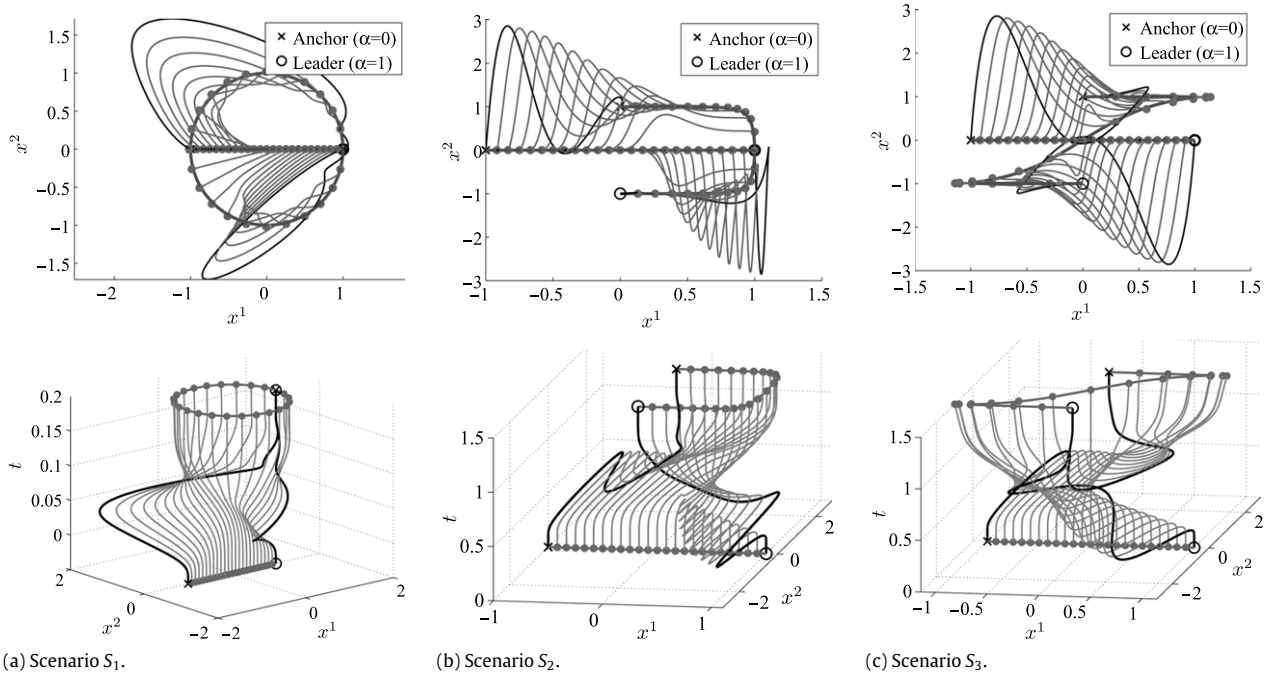

(a) Scenario S_1. (b) Scenario S_2. (c) Scenario S_3.

Fig. 4. Agent trajectories in the (x^1, x^2)-plane (top) and (x^1, x^2, t)-domain (row) for the scenarios of Table 1. Black lines correspond to the anchor (×) and leader (○) trajectories, gray lines represent the followers motions (•).

Table 1
System and summation parameters and stationary anchor and leader positions at $t = T$ for the evaluation of (2). The notion '—' in the parameters ξ^j and k^j refers to partial summation. In all scenarios $N^j = 48$ series coefficients were used.

Sc.	Fig.	a^1/a^2	b^1/b^2	$(\bar{c}^{1,0}, \bar{c}^{1,1})/(\bar{c}^{1,0}, \bar{c}^{2,1})$	ξ^1/ξ^2	k^1/k^2	T^1/T^2	T_c^1/T_c^2	$(\bar{u}_a^{1,1}, \bar{u}_a^{2,1})$	$(\bar{u}_l^{1,1}, \bar{u}_l^{2,1})$
S_1	4(a)	1/1	0/0	$(0, 4\pi^2)/(0, 4\pi^2)$	−/−	−/−	0.25/0.25	0.25/0.25	(1, 0)	(1, 0)
S_2	4(b)	1/0.05	0/1	$(0, \pi^2)/(0, 0)$	−/5	−/1	1.5/1.5	1.5/1.5	(0, 1)	(0, −1)
S_3	4(c)	1/0.05	0/1	$(0, 4\pi^2)/(0, 0)$	−/5	−/1	1.5/1.5	1.5/1.5	(0, 1)	(0, −1)

achieved, which both illustrates and confirms the rather broad variety of achievable deployment profiles by means of the proposed PDE-based motion planning approach. The evolving small deviations in Fig. 4(c) between the desired and the achieved final formation are due to the discretized setting, which serves as the model for the feedforward formation control design.

Remark 6. Applying spectral analysis implies that the linear PDE with $c^1(t) = \bar{c}^{1,1} = 4\pi^2$ for $t \geq t_0 + T$ governing the x^1- and x^2-motion in scenario S_1 and the x^1-motion in scenario S_3 is unstable. This, however, does not influence the simulation results for the feedforward formation control in the considered time frame and confirms the accuracy, which is achievable using the presented PDE-based motion planning approach. In view of applications, a suitable feedback control has to be integrated, e.g., by making use of the backstepping approach (Frihauf & Krstic, 2009), whose design for the considered nonlinear time-varying setting is a topic of current research.

6. Conclusion

By modeling the collective leader–follower dynamics of a continuum of agents in terms of two decoupled modified time-varying Burgers equations with the boundary conditions corresponding to the anchor and leader agent positions serving as the control inputs, a systematic solution to the motion planning problem is proposed for the deployment of mobile agents into desired formation profiles in the plane. For this, formal power series are used to determine a differential parametrization of any system variable in terms of a basic output. The uniform convergence with a finite radius of convergence of the parametrized series can be verified for time-varying system parameters and desired trajectories for the basic output from a certain but broad Gevrey class of non-analytic functions. Moreover, a significantly enhanced domain of applicability is achieved by incorporating appropriate summation methods and generalized sequence transformation, which also allow to sum certain divergent series to a meaningful limit, into the design process. With this, the suitable assignment of desired trajectories for the basic output directly yields the respective feedforward formation controls for the anchor and leader, which enable the realization of finite time transitions between desired deployment profiles from the set of steady state of the governing nonlinear PDEs. An appropriate choice of the time-varying system parameter, which serves as a degree of freedom, enables the transition between different families of steady states. The transfer of the agent continuum to a finite agent number is achieved by discretizing the PDE model. This directly implies a corresponding decentralized communication and interconnection structure for the multi-agent system, which is required to obtain the desired formation. Based on these results future work includes the combination of the proposed motion planning approach with suitable methods of stabilization (see, e.g., Meurer & Kugi, 2007, Frihauf & Krstic, 2009 for a backstepping approach) to enable the deployment into formations corresponding to unstable steady states.

Appendix A. Proof of Theorem 3

In the following, the super-script j referring to the individual directions $x^j(\alpha, t)$, $j = 1, 2$, and, whenever it is clear from the context, the explicit dependency on time is omitted for the sake

of clarity of presentation. For the proof of Theorem 3, two Lemmas are introduced.

Lemma 7. *For $y_1(t), y_2(t) \in G_{M,\varsigma}(\overline{\mathbb{R}_{t_0}})$ with $\varsigma \in [1,2]$ and $c(t)$ as in Assumption 2 the $\mathbb{N} \ni l$-th derivative of $\hat{x}_n(t)$, $n \geq 2$, satisfies*

$$|\partial_t^l \hat{x}_n| \leq M^{l+n}((l+n-1)!)^\varsigma F_n, \quad n \geq 2 \tag{A.1a}$$

with F_n determined recursively according to

$$F_n = \frac{1}{a}\left(\frac{\gamma_n F_{n-2}}{M(n-1)^\varsigma} + \frac{b}{M(n-1)^\varsigma}\sum_{i=0}^{n-3}\binom{n-2}{i}\frac{F_{n-2-i}F_{i+1}}{(\beta_i^n)^\varsigma} + b\frac{F_{n-1}F_0}{(n-1)^\varsigma}\right), \quad n \geq 3 \tag{A.1b}$$

and $F_0 = F_1 = 1, F_2 = (2+b)/a$, $\beta_i^n = \binom{n-2}{i+1}(i+1)$, and $\gamma_n = 1 + 1/(n-2)^\varsigma$.

Proof. Given $y_1 = \hat{x}_0$ and $y_2 = \hat{x}_1$, it follows from Definition 1 that $|\partial_t^l \hat{x}_0| \leq M^{l+1}(l!)^\varsigma$ and $|\partial_t^l \hat{x}_1| \leq M^{l+1}(l!)^\varsigma$. By means of the Leibniz formula the absolute value of the l-th derivative of $\hat{x}_n$, $n \geq 2$, as introduced in (5a) evaluates to

$$|\partial_t^l \hat{x}_n| \leq \frac{1}{a}\left[|\partial_t^{l+1}\hat{x}_{n-2}| + \sum_{p=0}^{l}\binom{l}{p}|\partial_t^{l-p}c||\partial_t^p \hat{x}_{n-2}| + b\sum_{i=0}^{n-2}\binom{n-2}{i}\sum_{p=0}^{l}\binom{l}{p}|\partial_t^{l-p}\hat{x}_{n-2-i}||\partial_t^p \hat{x}_{i+1}|\right].$$

A direct computation for $n = 2$ hence reveals $|\partial_t^l \hat{x}_2| \leq M^{l+2}((l+1)!)^\varsigma(2+b)/a$ which coincides with (A.1). Assuming that (A.1) holds for all $n = 2, 3, \ldots, N-1$, it follows that

$$|\partial_t^l \hat{x}_N| \leq \frac{1}{a}\left[|\partial_t^{l+1}\hat{x}_{N-2}| + \sum_{p=0}^{l}\binom{l}{p}|\partial_t^{l-p}c||\partial_t^p \hat{x}_{N-2}| + b\sum_{i=0}^{N-2}\binom{N-2}{i}\sum_{p=0}^{l}\binom{l}{p}|\partial_t^{l-p}\hat{x}_{N-2-i}||\partial_t^p \hat{x}_{i+1}|\right].$$

Due to the individual bounds for the derivatives of both $\hat{x}_0$ and $\hat{x}_1$ all terms involving $\hat{x}_0$ and $\hat{x}_1$ have to be treated separately, which for $N > 3$ results in

$$|\partial_t^l \hat{x}_N| \leq \frac{1}{a}\left[|\partial_t^{l+1}\hat{x}_{N-2}| + \sum_{p=0}^{l}\binom{l}{p}|\partial_t^{l-p}c||\partial_t^p \hat{x}_{N-2}| + b\sum_{p=0}^{l}\binom{l}{p}\left\{|\partial_t^{l-p}\hat{x}_{N-2}||\partial_t^p \hat{x}_1| + |\partial_t^{l-p}\hat{x}_0||\partial_t^p \hat{x}_{N-1}| + \sum_{i=1}^{N-3}\binom{N-2}{i}|\partial_t^{l-p}\hat{x}_{N-2-i}||\partial_t^p \hat{x}_{i+1}|\right\}\right].$$

By making use of (A.1a) and $c(t) \in G_{M,\varsigma}(\overline{\mathbb{R}_{t_0}})$, $\varsigma \in (1,2]$ from Assumption 2 as well as Lemmas 9 and 10 of Appendix B this inequality reduces to

$$|\partial_t^l \hat{x}_N| \leq M^{l+N}((l+N-1)!)^\varsigma \times \left[\frac{1}{a}\left(\frac{\gamma_N F_{N-2}}{M(l+N-1)^\varsigma} + b\left\{\frac{F_1 F_{N-2}}{M[(N-2)(l+N-1)]^\varsigma} + \frac{F_{N-1}F_0}{(N-1)^\varsigma} + \frac{1}{M(l+N-1)^\varsigma}\sum_{i=1}^{N-3}\binom{N-2}{i}\frac{F_{N-2-i}F_{i+1}}{(\beta_i^N)^\varsigma}\right\}\right)\right].$$

Since $l \geq 0$ the square bracketed term can be bounded from above to obtain

$$|\partial_t^l \hat{x}_N| \leq M^{l+N}((l+N-1)!)^\varsigma \left[\frac{1}{a}\left(\frac{\gamma_n F_{N-2}}{M(N-1)^\varsigma} + b\left\{\frac{F_1 F_{N-2}}{M[(N-2)(N-1)]^\varsigma} + \frac{F_{N-1}F_0}{(N-1)^\varsigma} + \frac{1}{M(N-1)^\varsigma}\sum_{i=1}^{N-3}\binom{N-2}{i}\frac{F_{N-2-i}F_{i+1}}{(\beta_i^N)^\varsigma}\right\}\right)\right].$$

Comparing the terms in square brackets with (A.1b) yields

$$|\partial_t^l \hat{x}_N| \leq M^{l+N}((l+N-1)!)^\varsigma F_N$$

which completes the proof. □

Lemma 8. *The coefficients F_n defined in (A.1b) satisfy*

$$F_n \leq (A(M))^n \frac{n!}{((n-1)!)^\varsigma}, \quad n \geq 1 \tag{A.2}$$

with $A(M)$ given by (8).

Proof. Consider the mapping $G_n = F_n((n-1)!)^\varsigma/n!$, $n \geq 1$, which allows us to re-write the recursion (A.1b) in terms of G_n according to

$$G_n = \frac{1}{a}\left(\frac{\gamma_n(n-2)^\varsigma}{Mn(n-1)}G_{n-2} + \frac{b}{n}G_{n-1} + \frac{b}{Mn(n-1)}\sum_{i=0}^{n-3}(i+1)G_{i+1}G_{n-2-i}\right) \tag{A.3a}$$

for $n \geq 3$ with the two starting conditions

$$G_1 = 1, \qquad G_2 = \frac{2+b}{2a}. \tag{A.3b}$$

It is subsequently shown by induction that

$$G_n \leq (A(M))^n, \quad n \geq 1 \tag{A.4}$$

with $A(M)$ from (8). For the induction start consider $n = 1$ and $n = 2$, i.e, $A(M) = 1$ and $A^2(M) = (2+b)/(2a)$, which directly yield the first two arguments on the right hand side of (8). Under the assumption that (A.4) holds for all $n = 1, 2, \ldots, N-1$, it follows with (A.3) for $N \geq 3$ that

$$G_N \leq (A(M))^N \underbrace{\frac{1}{a}\left(\frac{2}{M(A(M))^2} + \frac{b}{3A(M)} + \frac{b}{2MA(M)}\right)}_{=g(A(M))}$$

since $(N-2)^\varsigma/(N(N-1)) \leq 1$ if $\varsigma \in [1,2]$, $1/N \leq 1/3$, and $(N-2)/(2N) \leq 1/2$ as well as $\gamma_N \leq 2$ for $N \geq 3$. Solving the quadratic equation $g(A(M)) = 1$ for $A(M)$ and taking the larger value together with the results for $n = 1$ and $n = 2$ results in (8). □

With Lemmas 7 and 8, the proof of Theorem 3 follows immediately from the Cauchy–Hadamard Theorem.

Proof. By taking into account Lemma 7 for $l = 0$ and Lemma 8 for the growth of the coefficients F_n the supremum of the series coefficients $\hat{x}_n$, $n \in \mathbb{N}$, satisfies

$$\hat{X}_n := \sup_{t \geq 0}|\hat{x}_n| \leq (MA(M))^n n!, \quad n \geq 2 \tag{A.5}$$

for $\varsigma \in [1, 2]$ and $A(M)$ as introduced in (8). By the Cauchy–Hadamard Theorem, the radius of convergence ρ of the power series (4) is given by $\rho = (\lim_{n\to\infty} |\hat{X}_n/n!|^{1/n})^{-1}$. In view of (A.5), this yields a finite radius of convergence $\rho \geq 1/(MA(M))$ such that the series (4) with coefficients (A.5) converges for all compact subsets of $|\alpha - \hat{\alpha}| < 1/(MA(M))$, which completes the proof. □

Appendix B. Useful Lemmas

Lemma 9 (*Gevrey (1918)*). *Given $\varsigma \geq 1$ and $\lambda_n > 0$ for all $n \in \mathbb{N}$, then $\sum_{n=1}^{\infty}(\lambda_n)^{\varsigma} \leq (\sum_{n=1}^{\infty}\lambda_n)^{\varsigma}$.*

Lemma 10 (*Lynch and Rudolph (2002)*). *For all $k, l \in \mathbb{N}$, $\sum_{j=0}^{l}\binom{l}{j}(l-j)!\,(j+k)! = \sum_{j=0}^{l}\binom{l}{j}(l-j+k)!\,(j)! = \frac{(l+k+1)!}{k+1}$.*

References

Alvarez, L., Horowitz, R., & Li, P. (1999). Traffic flow control in automated highway systems. *Control Engineering Practice*, *7*, 1071–1078.

Balch, T., & Arkin, R. C. (1998). Behavior-based formation control for multirobot teams. *IEEE Transactions on Robotics Automation*, *14*(6), 926–939.

Balser, W. (2000). *Formal power series and linear systems of meromorphic ordinary differential equations*. Springer-Verlag.

Balser, W. (2001). Summability of formal power series solutions of ordinary and partial differential equations. *Functional Differential Equations*, *8*, 11–24.

Balser, W., & Braun, R. W. (2000). Power series methods and multisummability. *Mathematische Nachrichten*, *212*, 37–50.

Balser, W., & Miyake, M. (1999). Summability of formal solutions of certain partial differential equations. *Acta Scientiarum Mathematicarum. Univ. Szeged*, *65*, 543–551.

Barooah, P., Mehta, P. G., & Hespanha, J. P. (2009). Mistuning-based control design to improve closed-loop stability margin of vehicular platoons. *IEEE Transactions Automatic Control*, *54*(9), 2100–2113.

Bullo, F., Cortés, J., & Martínez, S. (2009). Distributed control of robotic networks. In *Applied mathematics series*. Princeton University Press.

Dunbar, W. B., & Murray, R. M. (2006). Distributed receding horizon control for multi-vehicle formation stabilization. *Automatica*, *42*(4), 549–558.

Ferrari-Trecate, G., Buffa, A., & Gati, M. (2006). Analysis and coordination in multi-agent systems through partial difference equations. *IEEE Transactions Automatic Control*, *51*(6), 1058–1063.

Fliess, M., Lévine, J., Martin, P., & Rouchon, P. (1995). Flatness and defect of non-linear systems: introductory theory and examples. *International Journal of Control*, *61*, 1327–1361.

Frihauf, P., & Krstic, M. Rapidly convergent leader-enabled multi-agent deployment into planar curves. In Proc. American control conference, pp. 1994–1999, St. Louis MO, USA, June 2009.

Gevrey, M. (1918). Sur la nature analytique des solutions des équations aux dérivées partielles. *Annales Scientifiques de l'Ecole Normale Superieure*, *25*, 129–190.

Hardy, G. H. (1964). *Divergent series* (3 ed.). Oxford at the Clarendon Press.

Kim, J. Y., Kim, K.-D., Natarajan, V., Kelly, S. D., & Bentsman, J. (2008). PDE-based model reference adaptive control of uncertain heterogeneous multiagent networks. *Nonlinear Analysis: Hybrid Systems*, *2*, 1152–1167.

Krstic, M., Magnis, L., & Vazquez, R. (2008). Nonlinear stabilization of shock-like unstable equilibria in the viscous burgers PDE. *IEEE Transactions Automatic Control*, *53*(7), 1678–1683.

Krstic, M., Magnis, L., & Vazquez, R. (2009). Nonlinear control of the viscous Burgers equation: Trajectory generation, tracking, and observer design. *Journal of Dynamic Systems, Measurement and Control*, *131*, 021012.

Krstic, M., & Smyshlyaev, A. (2008). *Boundary control of PDEs: A course on backstepping designs*. SIAM.

Lynch, A. F., & Rudolph, J. (2002). Flatness-based boundary control of a class of quasilinear parabolic distributed parameter systems. *International Journal of Control*, *75*(15), 1219–1230.

Meurer, T. Feedforward and feedback tracking control of diffusion–convection–reaction systems using summability methods. Fortschr.-Ber. VDI Reihe 8 Nr. 1081. VDI Verlag, Düsseldorf, 2005. Available as electronic dissertation at http://elib.uni-stuttgart.de/opus/volltexte/2006/2736/.

Meurer, T., & Kugi, A. Tracking control for a diffusion–convection–reaction system: combining flatness and backstepping. In Proc. 7th IFAC symposium nonlinear control systems NOLCOS 2007, pp. 583–588, Pretoria SA, Aug. 21–24 2007.

Meurer, T., & Kugi, A. (2009). Trajectory planning for boundary controlled parabolic PDEs with varying parameters on higher-dimensional spatial domains. *IEEE Transactions on Automatic Control*, *54*(8), 1854–1868.

Meurer, T., & Zeitz, M. (2005). Feedforward and feedback tracking control of nonlinear diffusion–convection–reaction systems using summability methods. *Industrial & Engineering Chemistry Research*, *44*, 2532–2548.

Meurer, T., & Zeitz, M. (2008). Model inversion of boundary controlled parabolic partial differential equations using summability methods. *Mathematical and Computer Modelling of Dynamcial Systems*, *14*(3), 213–230.

Murray, R. M. (2007). Recent research in cooperative control of multivehicle systems. *Journal of Dynamic Systems, Measurement and Control*, *129*, 571–583.

Olfati-Saber, R. (2006). Flocking for multi-agent dynamic systems: algortihms and theory. *IEEE Transactions Automatic Control*, *51*(3), 401–420.

Olfati-Saber, R., & Murray, R. M. (2004). Consensus problems in networks of agents with switching topology and time-delays. *IEEE Transactions Automatic Control*, *49*(9), 1520–1533.

Petit, N., & Rouchon, P. (2002). Dynamics and solutions to some control problems for water-tank systems. *IEEE Transactions on Automatic Control*, *47*(4), 594–609.

Ren, W., & Beard, R. W. (2004). Formation feedback control for multiple spacecraft via virtual structures. *IEE Proceedings*, *151*(3), 357–368.

Ren, W., & Beard, R. W. (2008). *Distributed consensus in multi-vehicle cooperative control*. London: Springer-Verlag.

Rodino, L. (1993). *Linear partial differential operators in Gevrey spaces*. Singapore: World Scientific Publishing Co. Pte. Ltd.

Sarlette, A., & Sepulchre, R. A PDE viewpoint on basic properties of coordination algorithms with symmetries. In Proc. IEEE Conference on Decision and Control CDC, pp. 5139–5144, 2009.

Weniger, E. J. (1989). Nonlinear sequence transformations for the acceleration of convergence and the summation of divergent series. *Computer Physics Reports*, *10*, 189–371.

Zhang, W., & Hu, J. (2008). Optimal multi-agent coordination under tree formation constraints. *IEEE Transactions Automatic Control*, *53*(3), 692–705.

Thomas Meurer received the diploma in chemical engineering from the University of Stuttgart, Germany in 2001 and the M.S. in engineering science and mechanics from the Georgia Institute of Technology, Atlanta, USA in 2000. He received the Ph.D. degree from the University of Stuttgart in 2005. From 2005 to 2007 he was a post-doc with the Chair of System Theory and Automatic Control at the Saarland University in SaarbrÃ1/4cken, Germany, and in 2007 he joined the Automation and Control Institute at the Vienna University of Technology, Austria, as a senior researcher and as the leader of the distributed-parameter systems group. His research interests include the feedback control and the trajectory planning for linear and nonlinear distributed-parameter systems, differential flatness, nonlinear control theory and observer design, multi-agent networks, and computational methods in control. He serves as Associate Editor for the IFAC Control Engineering Practice.

Miroslav Krstic holds the Alspach endowed chair and is the founding Director of the Cymer Center for Control Systems and Dynamics at University of California, San Diego. He is a co-author of eight books on nonlinear control, adaptive control, control of PDE and delay systems, control of turbulent fluid flows, stochastic nonlinear systems, and extremum seeking. Krstic has held the Springer Distinguished Visiting Professorship at UC Berkeley and is a recipient of the PECASE, NSF Career, and ONR Young Investigator Awards, as well as the Axelby and Schuck Paper Prizes. Krstic was the first recipient of the UCSD Research Award in the area of engineering. He is a Fellow of IEEE and IFAC and serves as Senior Editor in Automatica and IEEE Transactions on Automatic Control.